Journal of Materials and Manufacturing (2022) 2: 41-52

Journal of Materials and Manufacturing

J-V and C-V characteristic of CdS/CdTe solar cell modelled by SCAPS-1D program

Sami Dursun[a], Serap Yiğit Gezgin[b] and Hamdi Şükür Kılıç[b,c] *

[a]*Department of Metallurgical and Materials Engineering, Konya Technical University, Konya 42031, Turkey*
(ORCID: 0000-0002-4581-4900), samidursun@ktun.edu.tr
[b]*Department of Physics, Faculty of Science, University of Selcuk, Konya 42031, Turkey*
(ORCID: 0000-0003-3046-6138), serap3207@gmail.com
[c]*Laser Induced Proton Therapy Application and Research Center, University of Selcuk, Konya 42031, Turkey*
(ORCID: 0000-0002-7546-4243), hamdisukurkilic@selcuk.edu.tr

Abstract

In this spectacular work, we have theoretically modelled and experimentally produced a CdS/CdTe thin film heterojunction solar cell using some physical parameters of CdS thin film at 150 nm thickness and a 2.4 eV band gap. The photovoltaic (PV) characteristics of simulated solar cell PV have been determined based on a variety of variables. A spike-like conduction band offset has been formed between CdS and CdTe semiconductors. The PV performance has been negatively impacted (the variation of PV parameters for N_t variation in 10^{10}-10^{18} cm^{-3}) by some increases in operating temperature, Auger electron recombination coefficient and interface defect density (Nt). It has been observed and interpreted that the efficiency of solar cell is increased as the donor defect density (N_D) in CdS thin film increases. However, as N_D is increases, the capacitance is slightly decreased, and the voltage built in (V_{bi}) is also slightly increased. However, the conversion efficiency of solar cell is unaffected by this reduction in capacitance.

Keywords: CdS, CdTe, thin film, solar cell, SCAPS-1D simulation.

1. Introduction

The increasing demand for energy, as well as the use of fossil fuels as fuel, causes some serious environmental damages. This situation has led to a tendency toward to some alternative energy sources. One of these energy sources is solar PV source, which is the most popular renewable energy source. The fact that this resource is freely available in nature, reliable and cost-effective encourages significant research and development [1, 2]. Although silicon (Si)-based solar cells are the most widely available on the commercial market, some challenges still exist, such as flexibility, bulk, Si sheet expense and costly fabrication equipment [3-5].

Due to some stated limitations of Si-based PV devices, the focus has been on the production of alternative thin-film materials with high efficiency, low production cost and environmental friendliness [6-8]. The most promising materials preferred for obtaining thin films of this type are II-VI based compounds [9, 10]. When it comes to II-VI based compounds, the first materials, that come to mind, are CdTe and CdS and solar cells based on these materials have had a very important place in PV energy conversion in recent years [11]. CdTe thin-film-based solar cells have received much attention due to their low cost, high efficiency and reliable properties [7, 12-14]. A CdTe thin-film-based PV device achieved a power conversion efficiency of about 22%, comparable to that of crystalline Si solar cells. CdTe thin films have the advantages of having a low energy gap of about 1.5 eV and almost 100% of the incident photons having an energy greater than the band gap, being reliable, stable, and exhibiting high efficiency [15-17]. CdS is an n-type semiconductor with a band gap of 2.4 eV and exhibits high photoconductivity and has low electrical resistivity [18].

* Corresponding author.
E-mail addresses: hamdisukurkilic@selcuk.edu.tr
DOI: 10.5281/zenodo.7472259
Received: 2 December 2022, Revised: 16 December 2022 and Accepted: 19 December 2022
ISSN: 2822-6054

Considering some significant studies carried out based on CdS/CdTe heterojunction so far, Bonnet and Rabenhorst have conducted a study for the first time and they have achieved an experimental cell efficiency of 6% at the end of this study [19]. In another study, Britt and Ferekides have achieved 15.8% efficiency with glass/FTO/CdS/CdTe heterojunction [20]. Samoilenko *et al.* have achieved 16% efficiency by using a CdTe solar energy device with a reactive sputtering magnesium zinc oxide emitter in their work reported in the literature [13]. An efficiency of 22.1% has been obtained by researching CdTe, thin-film solar cells [21].

Studies of CdS/CdTe heterojunction solar cells can be determined experimentally as well as theoretically. One-dimensional Solar Cell Capacitance Simulator (SCAPS-1D) program is used to compare PV performances between a standard thin-film cadmium sulfide (CdS)/cadmium telluride CdTe solar cell and the proposed solar cell. This program is a graphical solar cell simulation program developed by Professor Marc at the Department of Electronics and Information Systems (ELIS) at the University of Gent in Belgium with LabWindows/CVI of National Instruments [22]. The SCAPS-1D simulation tool offers the ability to solve the fundamental equations of the semiconductor, including the Poisson, continuity, and electron and hole transport equations. The current-voltage (J-V) curve of a PV device, ac characteristics such as capacitance-voltage (C-V) and capacitance-frequency (C-f) and spectral response quantum efficiency) can also be interpreted with the simulator. Tinedert *et al*., in the numerical study carried out by them, the efficiency of theoretically designed CdS/CdTe heterojunction solar cell at room temperature has been calculated at 23.01 percent [23]. Regarding to CdS/CdTe heterojunction solar cell, Shah *et al*. have reported a power conversion efficiency of 19.18% in another numerical study [24].

Considering thin films as a relatively new system, their work could offer much broader opportunities for the technological developments in PV energy converters. Therefore, in this study, we modeled a CdS/CdTe heterojunction solar cell using CdS thin film that we have produced experimentally in our previous study. We have used SCAPS-1D program to investigate and optimize some changes in PV performance of solar cell. in order to achieve superior PV performances, solar cell output parameters can be evaluated by adapting some physical parameters of different layers, including operating temperatures, back contact operating function and surface recombination rates.

2. Material and Method

2.1. Numerical Modelling and Material Parameters

By using SCAPS-1D software, PV parameters of solar cells have been calculated by courtesy of some other physical parameters such as dielectric permittivity, band gap, electron affinity of semiconductor layers in solar cells, work function of contacts. All calculations within the scope of the study have been discussed in detail in our previous studies [25].

3. Results and Discussion

3.1. The modelling of CdS/CdTe thin film solar cells, using SCAPS-1D simulation program

The SCAPS-1D modelling tool has been used to model a Mo/p-CdTe/n-CdS/i-ZnO/AZO thin film solar cell in this study, as shown in Fig. 1. Molybdenum (Mo) is back contact, p-CdTe (Cadmium Telluride) is the absorber (active) semiconductor, CdS are an n-type semiconductor [26], i-ZnO (intrinsic-Zinc Oxide) is a transparent oxide semiconductor with a high resistance and AZO (Aluminium doped Zinc Oxide) is also a transparent conductive oxide semiconductor (front electrode).

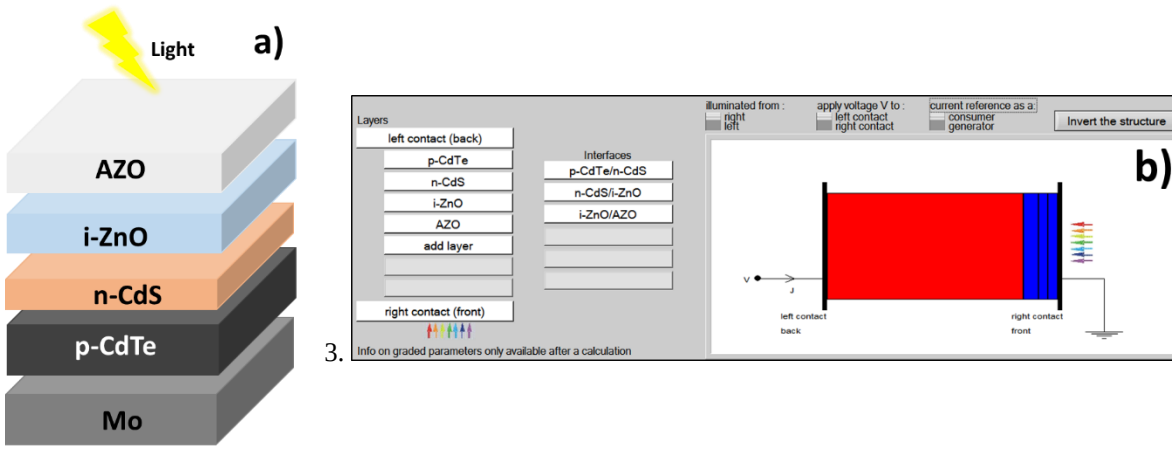

Fig. 1. (a) The schematic diagram and (b) the modelled structure of CdS/CdTe heterojunction thin film solar cell

In a previous study [27], we have used PLD approach to experimentally generate a thin film of CdS with a thickness of 150 nm and a band of 2.4 eV. This CdS thin film has been used in this investigation as an n-type semiconductor in a p-n heterojunction thin film solar cell. The simulation program receives the thickness, band gap and absorption coefficient file of CdS thin film [27-34]. Equation of $\alpha = 2.303 * (\frac{A}{W})$ is used to get the thin film absorption coefficient [35, 36]. Here, α is the absorption coefficient, A is the absorption, W is the film thickness. The program's absorption coefficient for CdS thin film was entered after the absorption coefficient was calculated using the unit m^{-1}. Table 1 lists some physical characteristics of layers in solar cell.

Table 1. The physical parameter of the layer formed the CdS/CdTe thin film solar cells

Layers	AZO	i-ZnO	n-CdS[37]	p-CdTe
Band Gap (eV)	3.3	3.3	2.4	1.45
Electron affinity (eV)	4.6	4.6	4.4	3.9
Dielectric permittivity (relative)	9	9	10	10.00
CB effective density of states (cm^{-3})	$2.20x10^{18}$	$2.20x10^{18}$	$1.80x10^{18}$	$9.20x10^{17}$
VB effective density of states (cm^{-3})	$1.80x10^{19}$	$1.80x10^{19}$	$2.40x10^{19}$	$5.20x10^{18}$
Electron/Hole thermal velocity (cm/s)	$1.00x10^{7}$	$1.00x10^{7}$	$1.00x10^{7}$	$1.00x10^{7}$
Electron/Hole mobility (cm^2/Vs)	100/25	100/25	100/25	320/40
Shallow donor density (cm^{-3})	$1.00x10^{20}$	$1.00x10^{5}$	variable	0
Shallow acceptor density (cm^{-3})	0	0	0	$1.0x10^{14}$
Thickness	100 nm	100 nm	150 nm	2 µm

Contacts	Back Contact (Mo)
Metal work function(eV)	5.00
Surface recombination velocity of electrons (cm/s)	$1\times10^{+5}$
Surface recombination velocity of holes (cm/s)	$1\times10^{+7}$

According to the energy band diagram in Fig. 2, a spike like Conduction Band Offset (CBO) was formed between CdS (2.4 eV band gap) and CdTe (1.45 eV band gap) semiconductors [38]. These results are in agreement with previous experimental results [39]. Such a configuration allows electrons to recombine at the interface as they switch from CdTe conduction band to CdS conduction band. This can limit an ideal charge transfer in a solar cell and result in lower charge aggregation. However, a partially ohmic structure is formed between the back Mo contact area and CdTe semiconductor. Thus, an ideal charge transfer can occur between the metal and CdTe, resulting in high currents in solar cell.

3.1.1. The energy band diagram of the CdS/CdTe heterojuction thin film solar cells

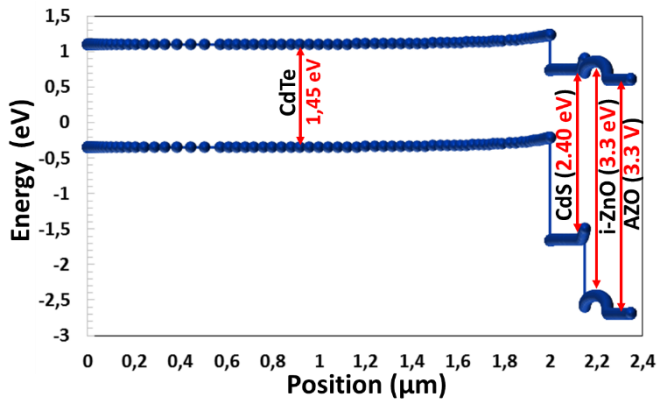

Fig. 2. The CdS/CdTe heterojunction thin film solar cell's energy band diagram

3.1.2. The effect of the interface defect density of (N_t) of the PV parameters of CdS/CdTe heterojunction solar cell

The defects between n-CdS and p-CdTe semiconductors act as recombination points for charge carriers. These deficiencies, which contribute to Shockley-Read Hall (SHR) recombination, are situated close to the band edges because the carrier is likely to return to the appropriate bands for shallow levels [27, 40]. By decreasing charge aggregation in the depletion zone, this recombination has a negative impact on the performance of solar cells. The variation of PV parameters for N_t variation in 10^{10}-10^{18} cm^{-3} that are shown in Fig 3 (a-d). While Nt value was increased from 10^{10} to 10^{18} cm^{-3}, the open circuit voltage (V_{oc}), the short circuit current density (J_{sc}), Fill Factor (FF) and the power conversion efficiency (η) , PV parameters that decreased from 0.779 V to 0.529 V, from 34.9986 mA/cm^2 to 12.6524 mA/cm^2, form 60.8% to 51.71% and from 20.74% to 4.33%, respectively. But these PV parameters are almost stable between 10^{17} cm^{-3}-10^{18} cm^{-3}. J-V characteristics in Fig. 3e shows that as Nt rises from 10^{10} cm^{-3}-10^{16} cm^{-3}, Jsc and Voc parameters decrease significantly. Since PV values for 10^{17} cm^{-3} and10^{18} cm^{-3} are very close to that for10^{16} cm^{-3} and overlap, they are not shown on J-V curve.

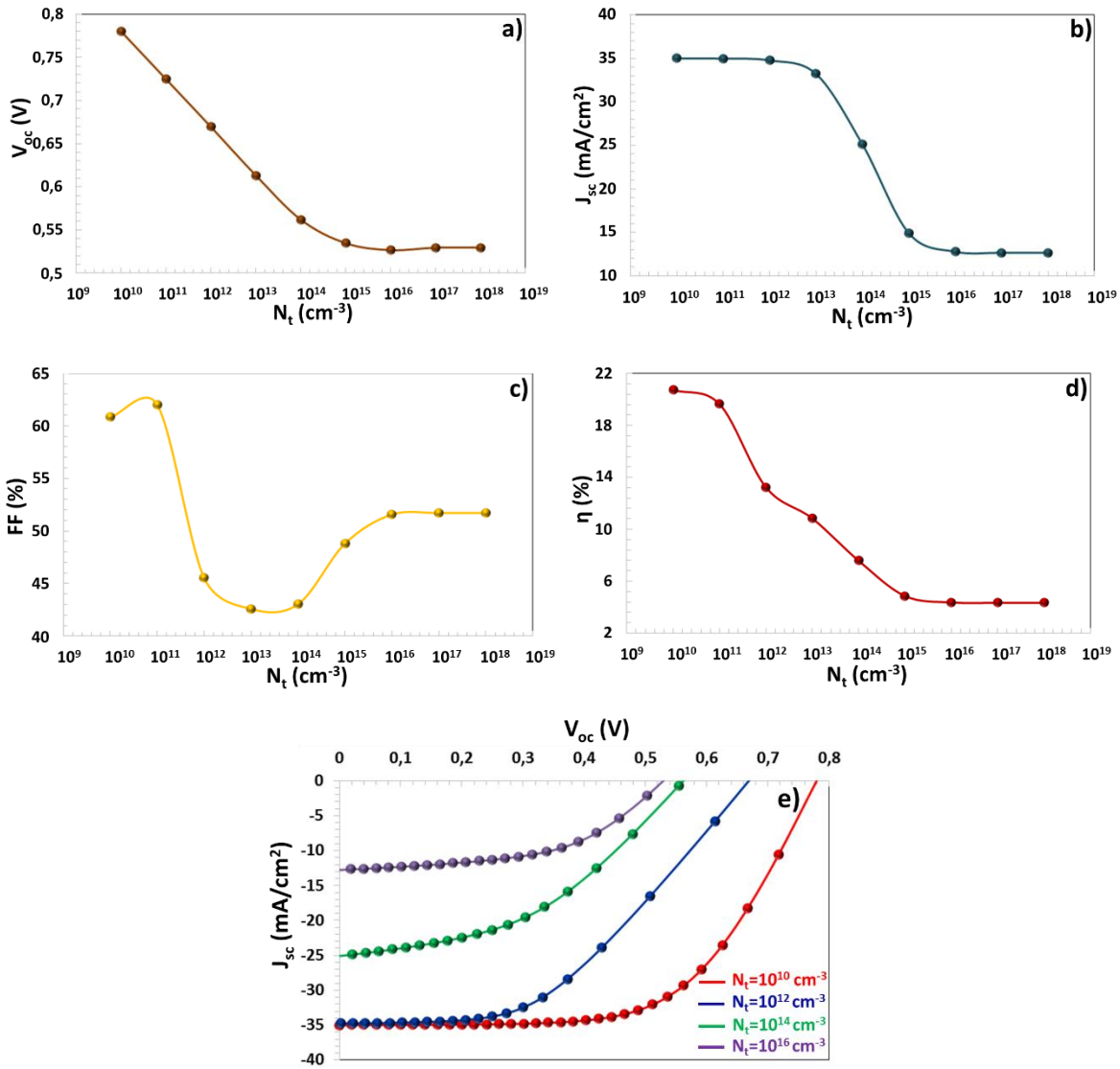

Fig. 3. (a-d) The PV parameters vs N_t (interface defect density) of CdS/CdTe thin film solar cell **e)** J-V characteristic for N_t

3.1.3. The effect of the donor defect density of (N_D) of CdS thin film on the PV parameters of the heterojunction solar cell

The effect of N_D value in 1.10^{17} cm^{-3} and 9.10^{17} cm^{-3} range on PV parameters of CdS/CdTe solar cell is presented in Fig. 4. N_D value in band diagram boosts an n-type features of CdS thin film by increasing the number of significant charge carriers in this thin film [41, 42]. V_{oc}= 0.731 V, J_{sc}=34.9331 mA/cm^2, FF=45.15% and η=14.43% for 1.10^{17} cm^{-3} of N_D were enhanced to V_{oc}= 0.779 V, J_{sc}=34.9660 mA/cm^2, FF=48.20% and η=16.43% for 9.10^{17} cm^{-3} of N_D [43]. Thus, as the number of major charges in CdS enhances with an increase in N_D, charge collection from the depletion side increases and possible recombination is overcome. As seen in Fig 4e, while there was no significant change in Jsc, a clear increament was observed in V_{oc} and based on N_D values, PV characteristics of CdS/CdTe solar cells is improved.

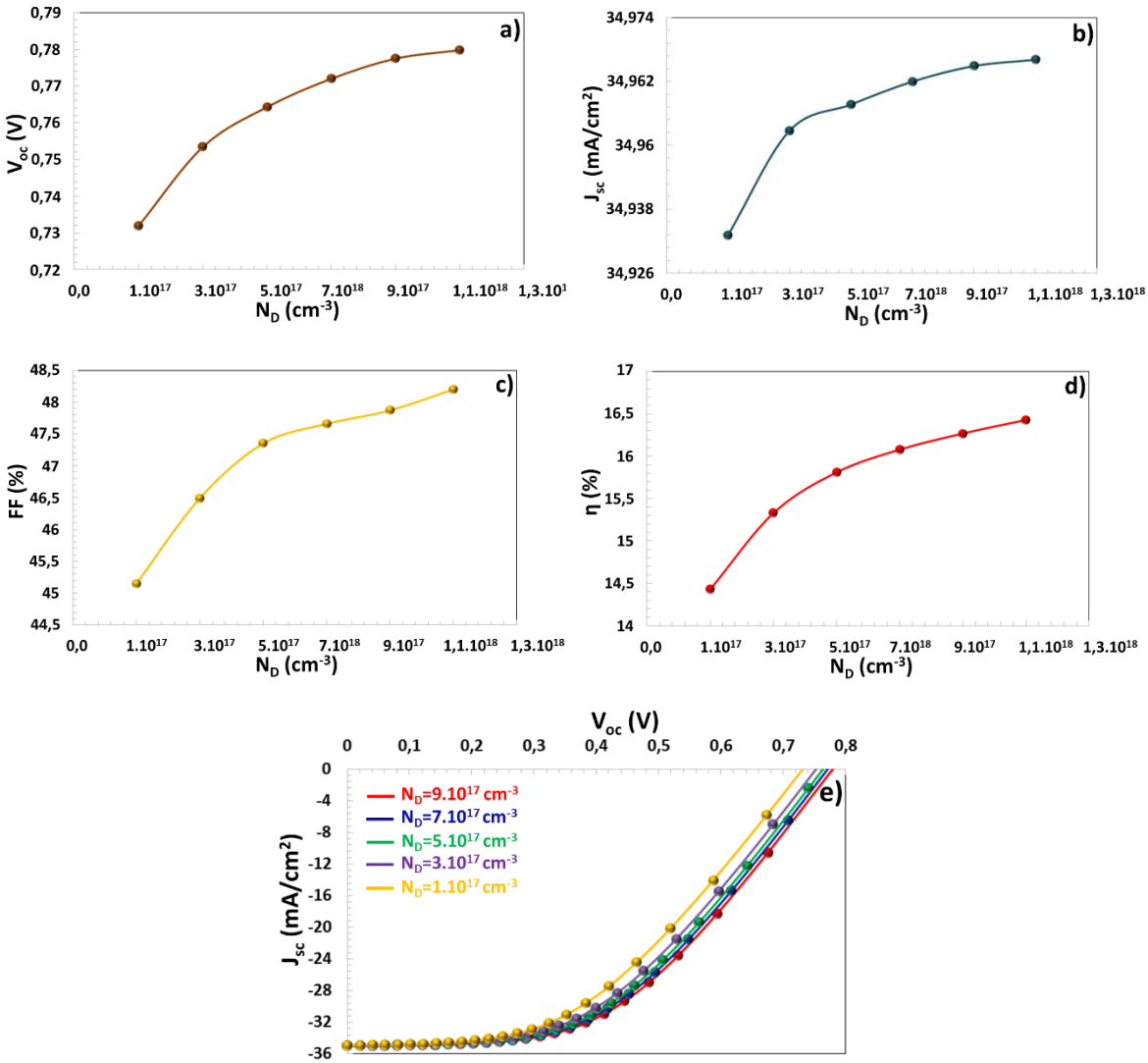

Fig. 4. (a-e) The influence of the heterojunction solar cell's PV parameters on the donor defect density (N_D) of CdS thin film

3.1.4. Auger electron capture coefficient's effect on on CdS/CdTe heterojunction solar cell

Fig.5 indicates that the effect of Auger electron capture coefficient (AECC) on PV parameter of CdS/CdTe solar cell. When electrons and holes recombine, the generated excess energy is not transferred to photons, but to electrons and holes to be excited to higher energy states in the same band [44, 45]. No radiation occurs in this process and the event is called as Auger recombination. For AECC, in the range of 10^{-32} and 10^{-28} cm^6/s, all PV parameters have not changed significantly, but when AECC was increased from 10^{-28} cm^6/s to 10^{-24} cm^6/s, V_{oc}, J_{sc} and η have decreased from 0.779 V to 0.752 V and from 34.966 mA/cm^2 to 17.622 mA/cm^2 and from 16.43% to 58.74%, respectively. AECC parameter was changed from 10^{-28} cm^6/s to 10^{-24} cm^6/s, FF was increased from 48.09% to 58.74%, respectively. The high probability of V and J values corresponding to the maximum power point on J-V characteristic may cause FF value to increase. In10^{-24} cm^6/s-10^{-20} cm^6/s range, all PV values have remained constant.

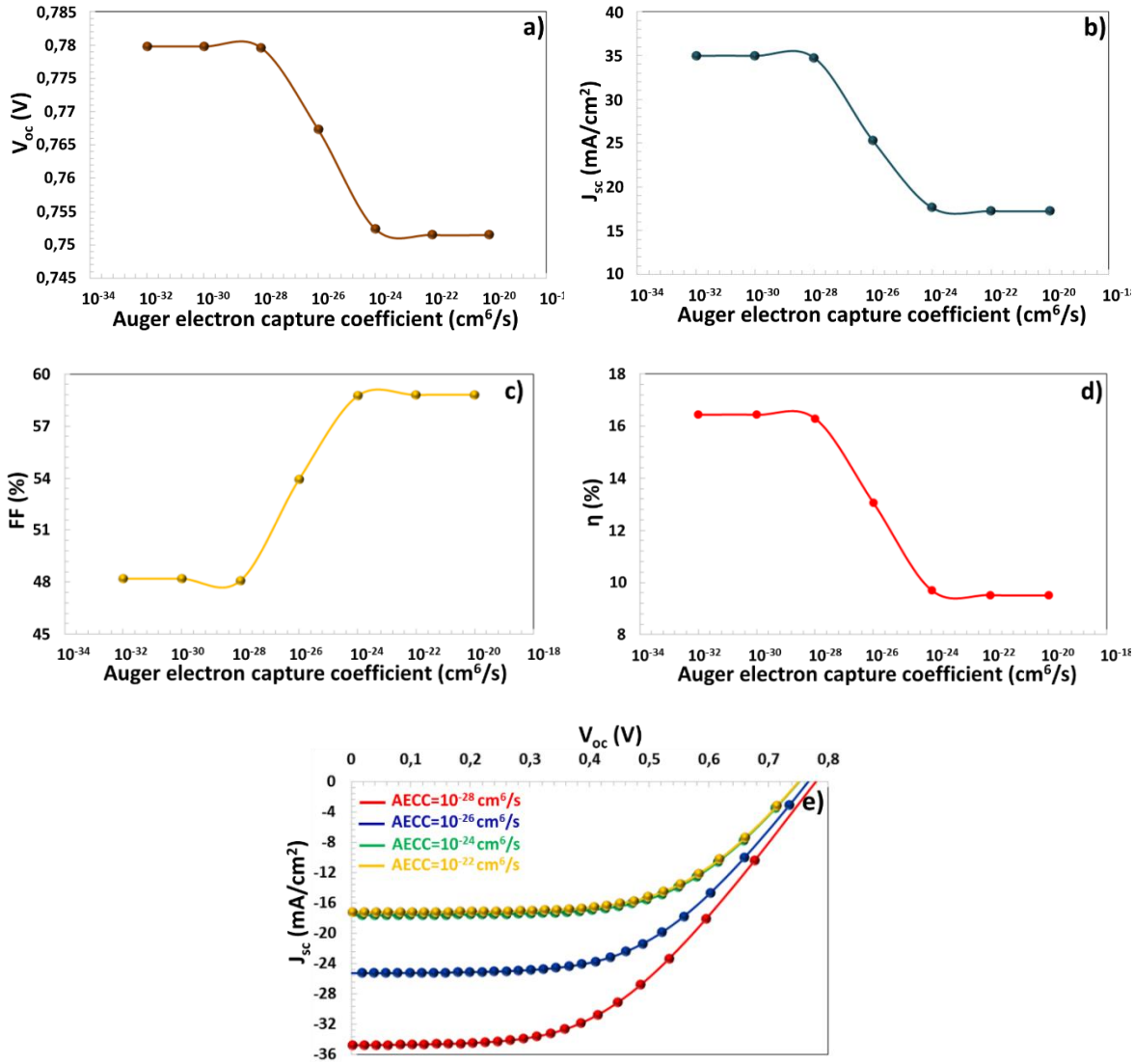

Fig. 5. (a-e) The effect of Auger electron capture coefficient on the PV parameters of CdS/CdTe solar cell

3.1.5. The PV characteristics of the CdS/CdTe thin film solar cells as a function of operation temperature

The operation temperature can adversely affect the performance of thin film solar cells. With some increase in the operation temperature, the band gap of semiconductor decreases and the voltage built in (V_{bi}) in the depletion region decreases [46, 47]. Also, charges become kinetic at high temperatures can become unstable and cause recombination. Thus, undesirable load transfers occur in the deposition region and the charge accumulation in the depletion region is lower, which causes the values of V_{oc}, J_{sc}, FF and the power conversion efficiency that decrease from 0.793 V to 0.718 V, from 34.979 mA/cm^2 to 34.968 mA/cm^2, from 48.06% to 46.41% and from 16.67% to 14.58%, respectively, while the operation temperature rises from 260 K to 360 K. Some decrease in the band gap and V_{bi} values causes a significant decrease in V_{oc} as shown in Fig. 6e.

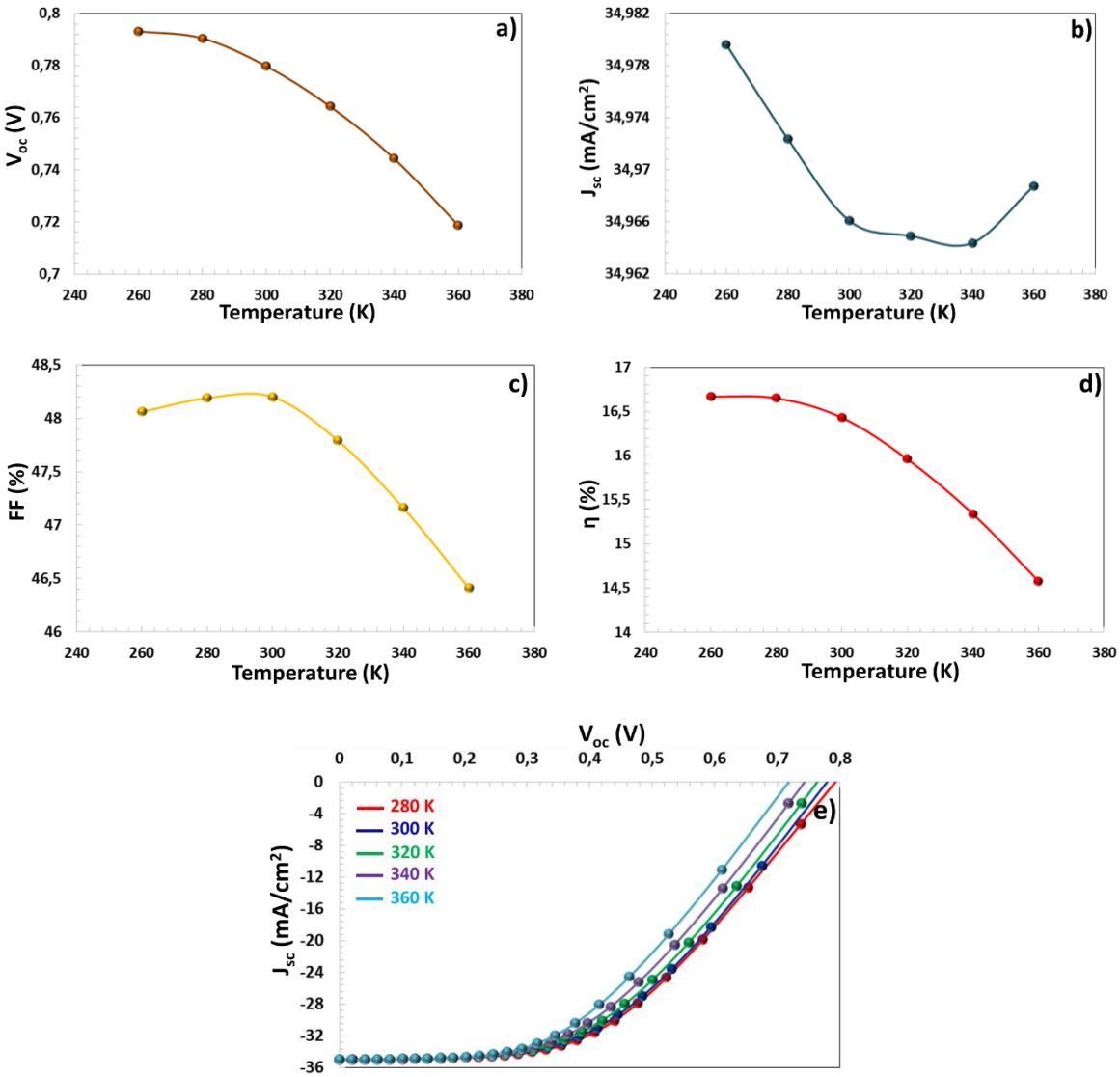

Fig. 6. (a-e) The PV characteristics of a CdS/CdTe thin film solar cell are affected by operation temperature

3.1.6. C-V characteristic of the CdS/CdTe solar cell and the effect of the donor defect density of (N_D) of CdS thin film on C-V characteristic of the solar cells

The C-V characteristics (from -1V to +1 V) of CdS/CdTe thin film solar cell depending on donor defect density is given in Fig 7a. The depletion capacitance of p-n junction is expressed by Equation (Eq).(1)[48-50]:

$$C(V) = A\sqrt{\frac{q\varepsilon\varepsilon_o N}{2(V_{bi}-V)}} \quad (1)$$

where A is cross-section area of junction, ε_o is the permittivity of free space and ε is the dielectric constant of semiconductor, q is the charge of the electron, N is the carrier density, V is the applied potential, V_{bi} is the built voltage in the deplation region. In Fig. 6a, at zero bias potential, capacitances of CdS thin film solar cell

depending on N_D values that is given Table 2. $1/C^2$-V curve in Fig. 7b is obtained by Mott-Schottky Eq. (2) [48-50]:

$$\frac{1}{C^2} = \frac{2}{q\varepsilon\varepsilon_o A^2 N}(V_{bi} - V) \quad (2)$$

The diffusion potential in the forward bais region forms the built potential (V_{bi}). In Fig. 6b, the point where the straight line drawn from the slope of the curve in the forward bias region cuts on the potential axis that indicates V_{bi}. Thus, V_{bi} values in CdS/CdTe solar cell has been obtained from Fig. 7b that is presented in Table 2.

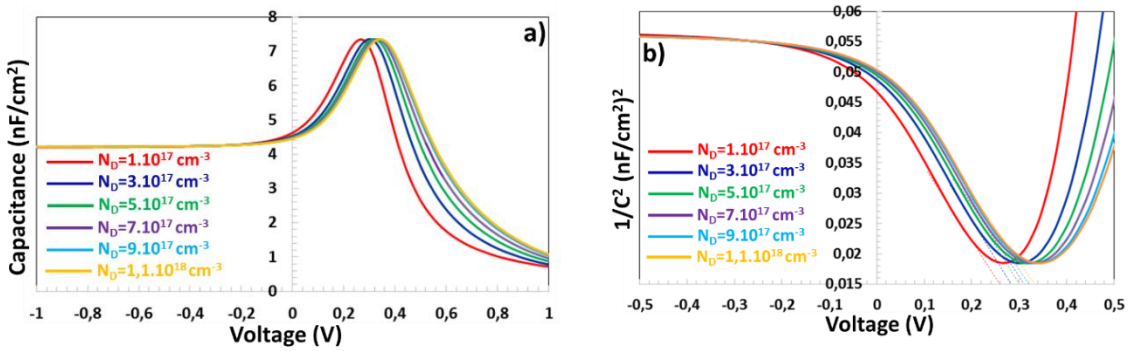

Fig. 7. (a) C-V characteristic and (b) Moss-Schotkky of the CdS/CdTe thin film solar cell

For zero bias voltage, while N_D values increases, the capacitance values of CdS/CdTe solar cell decreases and the built voltage increases [51]. In Table 2, Capacitance and V_{bi} values have been presented depending the donor defect density (N_D). With an increase in N_D value, the some decrease in capacitance indicates that a high number of donor defects are formed in CdS and this can lead to a partial reduction of the charge accumulation at the depletion site. However, since there is a minimum decrease in capacitance, it does not affect the efficiency of solar cell. Since V_{bi} is very low, some increase in V_{bi} isn't significantly affect the charge transitions, so it does not act to reduce the efficiency of solar cell.

Table 2. Capacitance and V_{bi} values depending the donor defect density (N_D)

Donor Defect Density (N_D)	Capacitance (nF/cm^2) at zero bias voltage	The built Voltage (V_{bi})
1.10^{17} cm^{-3}	4.62 nF/cm^2	0.26 V
3.10^{17} cm^{-3}	4.53 nF/cm^2	0.28 V
5.10^{17} cm^{-3}	4.49 nF/cm^2	0.30 V
7.10^{17} cm^{-3}	4.47 nF/cm^2	0.31 V
9.10^{17} cm^{-3}	4.46 nF/cm^2	0.32 V
$1,1.10^{18}$ cm^{-3}	4.45 nF/cm^2	0.33 V

4. Conclusion

In this study, we have modelled a CdS/CdTe heterojunction solar cell using CdS thin film that we have produced experimentally in our previous study. Spike like conduction band offset has occurred between

CdS/CdTe semiconductor. As an increase in N_t leads to recombination between CdS/CdTe semiconductors and the value of solar cell PV parameters has decreased. The increase in N_D value in CdS thin film improves PV performance of solar cell as it increases the number of major charges in this thin film. As the increase in operation temperature will reduce the band gap of the semiconductor and the voltage set-up in the depletion region, it causes undesired transitions and deterioration in PV performance. The increase in N_D slightly decreased the capacitance value and slightly increased the V_{bi} value.

Author Contribution Statement

Sami Dursun performed conceptualization, methodology, writing–original draft preparation, reviewing and editing; validation, investigation, resources, visualization; **Serap Yiğit Gezgin** performed data curation, writing–original draft preparation, methodology, investigation, resources, validation and **Hamdi Şükür Kılıç** performed writing–review & editing, visualization, investigation, supervision.

Acknowledgements

Authors kindly would like to thank,

- Selçuk University, High Technology Research and Application Center and

- Selçuk University, *Laser Induced Proton Therapy Application and Research Center* for supplying with Infrastructure and

- Selçuk University, Scientific Research Projects Coordination (BAP) Unit for grands via projects with references of 20401018 and 18401178.

References

[1] Yoon, J.-H., J. Song, and S.-J. Lee, Practical application of building integrated photovoltaic (BIPV) system using transparent amorphous silicon thin-film PV module. Solar Energy, 2011. 85(5): p. 723-733.
[2] Liu, C.P. and C.L. Chuang, Fabrication of copper–indium–gallium–diselenide absorber layer by quaternary-alloy nanoparticles for solar cell applications. Solar Energy, 2012. 86(9): p. 2795-2801.
[3] Green, M.A., et al., Solar cell efficiency tables (version 52). Progress in Photovoltaics: Research and Applications, 2018. 26(7): p. 427-436.
[4] Bhattacharya, S. and S. John, Beyond 30% conversion efficiency in silicon solar cells: a numerical demonstration. Scientific reports, 2019. 9(1): p. 1-15.
[5] Liu, Z., et al., Numerical and experimental exploration towards a 26% efficiency rear-junction n-type silicon solar cell with front local-area and rear full-area polysilicon passivated contacts. Solar Energy, 2021. 221: p. 1-9.
[6] Liang, G., et al., Spark plasma sintering of Sb2Se3 sputtering target towards highly efficient thin film solar cells. Solar Energy Materials and Solar Cells, 2020. 211: p. 110530.
[7] Powalla, M., et al., Thin-film solar cells exceeding 22% solar cell efficiency: An overview on CdTe-, Cu (In, Ga) Se2-, and perovskite-based materials. Applied Physics Reviews, 2018. 5(4): p. 041602.
[8] Romeo, A. and E. Artegiani, CdTe-based thin film solar cells: past, present and future. Energies, 2021. 14(6): p. 1684.
[9] Ghosh, B.K., et al., mcSi and CdTe solar photovoltaic challenges: Pathways to progress. Optik, 2020. 206: p. 164278.
[10] Petrus, R.Y., et al., optical properties of CdS thin films. Journal of Applied Spectroscopy, 2020. 87(1): p. 35-40.
[11] Kephart, J.M., R.M. Geisthardt, and W. Sampath, Optimization of CdTe thin-film solar cell efficiency using a sputtered, oxygenated CdS window layer. Progress in Photovoltaics: Research and Applications, 2015. 23(11): p. 1484-1492.

[12] Munshi, A.H., et al., Polycrystalline CdTe photovoltaics with efficiency over 18% through improved absorber passivation and current collection. Solar Energy Materials and Solar Cells, 2018. 176: p. 9-18.
[13] Samoilenko, Y., et al., Stable magnesium zinc oxide by reactive Co-Sputtering for CdTe-based solar cells. Solar Energy Materials and Solar Cells, 2020. 210: p. 110521.
[14] Manikandan, S., et al., Emerging nano-structured innovative materials as adsorbents in wastewater treatment. Bioresour. Technol., 2021. 320: p. 124394.
[15] Kumar, S.G. and K.K. Rao, Physics and chemistry of CdTe/CdS thin film heterojunction photovoltaic devices: fundamental and critical aspects. Energy & Environmental Science, 2014. 7(1): p. 45-102.
[16] He, F., et al., Characterization of sputtered MoOx thin films with different oxygen content and their application as back contact in CdTe solar cells. Vacuum, 2020. 176: p. 109337.
[17] Du, S., et al., Bilayered ZnTe/Cu1.4Te alloy thin films as a back contact for CdTe solar cells. Solar Energy, 2019. 185: p. 262-269.
[18] Rahman, S. and S.R. Al Ahmed, Photovoltaic performance enhancement in CdTe thin-film heterojunction solar cell with Sb2S3 as hole transport layer. Solar Energy, 2021. 230: p. 605-617.
[19] Bonnet, D. and H. Rabenhorst. New results on the development of a thin-film p-CdTe-n-CdS heterojunction solar cell. in Photovoltaic Specialists Conference, 9 th, Silver Spring, Md. 1972.
[20] Britt, J. and C. Ferekides, Thin-film CdS/CdTe solar cell with 15.8% efficiency. Applied physics letters, 1993. 62(22): p. 2851-2852.
[21] Green, M., et al., Solar cell efficiency tables. Progress in photovoltaics: research and applications, 2021. 29(1): p. 3-15.
[22] Burgelman, M.V. and J. Degrave, S.&Nollet. Modeling thin film PV devices. Prog. Photovolt. Res. Appl. 12: p. 143-153.
[23] Tinedert, I., et al., Design and simulation of a high efficiency CdS/CdTe solar cell. Optik, 2020. 208: p. 164112.
[24] Shah, D.K., et al., A simulation approach for investigating the performances of cadmium telluride solar cells using doping concentrations, carrier lifetimes, thickness of layers, and band gaps. Solar Energy, 2021. 216: p. 259-265.
[25] Gezgin, S.Y., Et Al., Modelling Of The Solar Cell Based On Cu2SnS3 Thin Film Produced By Spray Pyrolysis. Middle East Journal of Science. 8(1): p. 64-76.
[26] Rassol, R.A., R.F. Hasan, and S.M. Ahmed, Numerical Analysis of SnO2/Zn2SnO4/n-CdS/p-CdTe Solar Cell Using the SCAPS-1D Simulation Software. Iraqi Journal of Science, 2021: p. 505-516.
[27] Houimi, A., et al., Numerical analysis of CZTS/n-Si solar cells using SCAPS-1D. A comparative study between experimental and calculated outputs. Optical Materials, 2021. 121: p. 111544.
[28] Jamil, M., et al., Numerical modeling of AZTS as buffer layer in CZTS solar cells with back surface field for the improvement of cell performance. Solar Energy, 2022. 231: p. 41-46.
[29] Mishra, S.K., S. Padhy, and U.P. Singh, Silver incorporated bilayer Kesterite solar cell for enhanced device performance: A numerical study. Solar Energy, 2022. 233: p. 1-10.
[30] Darvishzadeh, P., H. Sohrabpoor, and N.E. Gorji, Numerical device simulation of carbon nanotube contacted CZTS solar cells. Optical and Quantum Electronics, 2016. 48(10): p. 480.
[31] Tousif, M.N., et al., Investigation of Different Materials as Buffer Layer in CZTS Solar Cells Using SCAPS. Journal of Clean Energy Technologies, 2018. 6(4): p. 293-296.
[32] Frisk, C., et al., Combining strong interface recombination with bandgap narrowing and short diffusion length in Cu2ZnSnS4 device modeling. Solar Energy Materials and Solar Cells, 2016. 144: p. 364-370.
[33] Haddout, A., et al., Influence of composition ratio on the performances of kesterite solar cell with double CZTS layers—A numerical approach. Solar Energy, 2019. 189: p. 491-502.
[34] Lam, N.D., Modelling and numerical analysis of ZnO/CuO/Cu2O heterojunction solar cell using SCAPS. Engineering Research Express, 2020. 2(2): p. 025033.
[35] Mustafa, F.A., Optical properties of NaI doped polyvinyl alcohol films. Physical Sciences Research International, 2013. 1(1): p. 1-9.
[36] Antar, E., Effect of γ-ray on optical characteristics of dyed PVA films. Journal of Radiation Research and Applied Sciences, 2014. 7(1): p. 129-134.

[37] Houimi, A., S. Yiğit Gezgin, and H.Ş. Kılıç, Theoretical Analysis of Solar Cell Performance with Different Backsurface-Filed Layers Utilizing Experimental Results of CdS Films Deposited by Pulsed Laser. physica status solidi (a), 2022: p. 2100780.
[38] Shiel, H., et al., Natural band alignments and band offsets of Sb2Se3 solar cells. ACS Applied Energy Materials, 2020. 3(12): p. 11617-11626.
[39] Yiğit Gezgin, S. and H.Ş. Kiliç, Determination of electrical parameters of ITO/CZTS/CdS/Ag and ITO/CdS/CZTS/Ag heterojunction diodes in dark and illumination conditions. Optical and Quantum Electronics, 2019. 51(11): p. 1-22.
[40] Meher, S., L. Balakrishnan, and Z. Alex, Analysis of Cu2ZnSnS4/CdS based photovoltaic cell: a numerical simulation approach. Superlattices and Microstructures, 2016. 100: p. 703-722.
[41] Hayakawa, T., et al., Control of donor concentration in n-type buffer layer for high-efficiency Cu (In, Ga) Se2 solar cells. IEEE Journal of Photovoltaics, 2018. 8(6): p. 1841-1846.
[42] Najm, A.S., et al., Numerical insights into the influence of electrical properties of n-CdS buffer layer on the performance of SLG/Mo/p-absorber/n-CdS/n-ZnO/Ag configured thin film photovoltaic devices. Coatings, 2021. 11(1): p. 52.
[43] Moon, M.M.A., et al., Design and simulation of FeSi2-based novel heterojunction solar cells for harnessing visible and near-infrared light. physica status solidi (a), 2020. 217(6): p. 1900921.
[44] Adewoyin, A.D., M.A. Olopade, and M. Chendo, Enhancement of the conversion efficiency of Cu2ZnSnS4 thin film solar cell through the optimization of some device parameters. Optik, 2017. 133: p. 122-131.
[45] Fu, H. and Y. Zhao, Efficiency droop in GaInN/GaN LEDs, in Nitride semiconductor light-emitting diodes (LEDs). 2018, Elsevier. p. 299-325.
[46] Tchognia, J.H.N., et al., Performances des cellules solaires à base de Cu2ZnSnS4 (CZTS): Une analyse par simulations numériques via le simulateur SCAPS. Afrique Science, 2015. 11(4): p. 16-23.
[47] Upadhyay, U., et al., Recent advances in heavy metal removal by chitosan based adsorbents. Carbohydr. Polym., 2021. 251: p. 117000.
[48] Pal, D. and S. Das, CV and IV characterisation of CdS/CdTe thin film solar cell using defect density model. Serbian Journal of Electrical Engineering, 2021. 18(2): p. 255-270.
[49] Echendu, O.K. and I.M. Dharmadasa, Graded-bandgap solar cells using all-electrodeposited ZnS, CdS and CdTe thin-films. Energies, 2015. 8(5): p. 4416-4435.
[50] Salari, M.A., et al. Effects Of the γ-radiation on the electrical characteristics of the Au/n-Si/Au-Sb Schottky diode. in Journal of Physics: Conference Series. 2016. IOP Publishing.
[51] Sawicka-Chudy, P., et al., Simulation of TiO2/CuO solar cells with SCAPS-1D software. Materials Research Express, 2019. 6(8): p. 085918.